

Estimation of the aspect-ratio distribution in chemically synthesized gold nanorods solution using UV-visible absorption spectroscopy

R Kumar^{1,2}, T H Nguyen², A Agrawal³, T Sun² and K T V Grattan²

² School of Mathematics, Computer Science and Engineering, City, University of London, London, EC1V 0HB, United Kingdom

³ Department of Engineering and Information Technology, University of Technology Sydney, 15 Broadway, Ultimo NSW 2007, Australia

E-mail: Rahul.Kumar@city.ac.uk

Abstract. A rapid and ubiquitous method to characterize samples of chemically synthesized Gold Nano Rods (GNRs) is by measuring their UV-visible spectra. The presence of transverse and longitudinal surface plasmon resonance peaks in UV-visible spectra indicate the presence of GNRs. However, the quality of the synthesised sample, and thus their performance in various sensor applications, depends on the geometrical variations of the GNRs present in the solution. As a result, an algorithm has been developed to estimate the Aspect Ratio (AR) variation of the GNRs present by theoretically fitting to the longitudinal surface plasmon resonance peak of the UV-visible spectrum. After numerically benchmarking has been undertaken, the developed algorithm has been used to calculate the mean and standard deviation of the ARs in two synthesized samples, showing that this method offers a fast and cost-effective alternative to Transmission Electron Microscopy.

1. Introduction

Gold nanorods (GNRs), due to their asymmetrical geometrical structure, exhibit two resonance peaks in the visible near-infrared (NIR) region [1]. The resonance corresponding to the shorter wavelength is known as Transverse Surface Plasmon Resonance (TR). It arises due to the oscillation of free electrons in the presence of an external electromagnetic wave along the width of the gold nanorods, whereas the resonance at the longer wavelength, known as Longitudinal Surface Plasmon Resonance (LR), is due to the oscillation of free electrons along their length. The ability to tune the LR of GNRs, over the range from the visible to the NIR wavelengths, by changing the Aspect Ratio (where AR is defined as length divided by width), has resulted in their being suited to many applications in diverse fields as cancer therapies, imaging, photovoltaic cells and LEDs [2]. Since the LR depends on the AR of the GNRs, it is important to know the distribution of the ARs in synthesized solution under investigation. Susie et al. [3] have shown that the broadening of the LR in the UV-visible spectrum can be used to determine the AR distribution, but however, their curve fitting technique used is cumbersome. Therefore, in this work, a curve fitting method using the Bellman principle of optimality to obtain a rapid estimate of the AR distribution in a colloidal solution has been developed and evaluated.

¹ To whom any correspondence should be addressed.



2. Methodology

2.1 Algorithm Used

As a first step in the automation of the process, the variables underpinning the modelled absorption coefficient of the GNRs, previously reported in the literature [3], were rearranged and represented as the product of two variables. The first variable contains the AR and the wavelength-dependent terms, represented by $A_{\lambda_x}^{AR}$. This is calculated for a given wavelength (λ_x) and AR and is known in present case. The second variable contains the number of particles per unit volume (contribution) of a given AR and needs to be determined. It is represented by N^{AR} . For a poly-dispersed colloidal solution, the resultant absorption at λ_x is the summation of the absorption coefficients of the individual ARs, as shown in Eq. (1).

$$A_{\lambda_x}^{AR^1} N^{AR^1} + A_{\lambda_x}^{AR^2} N^{AR^2} + \dots + A_{\lambda_x}^{AR^n} N^{AR^n} = A_{\lambda_x}^{exp}, \quad (1)$$

where, $A_{\lambda_x}^{AR}$ represents absorption of the n^{th} AR at wavelength λ_x , assuming the solution as mono-dispersed i.e. $N^{AR^1} = 1$. N^{AR^n} is the actual contribution of the n^{th} AR and needs to be calculated. $A_{\lambda_x}^{exp}$ is experimentally obtained absorption of the synthesized sample using UV-VIS absorption spectroscopy. Therefore, spanning the entire wavelength range of the LR, i.e. $\lambda_x > 615$ nm gives a set of overdetermined linear equations (ODE). This ODE set can be solved by using the Least Squares Approximation (LSA) method to find the unknown coefficient that is the contribution of the individual ARs. However, being unbounded in nature, the LSA approach may give a non-physical contribution, such as a result > 1 or a negative result. Therefore, to find the optimal bounded value of contribution i.e. that lying between 0 and 1, the Bellman Principal of optimality is used [4].

2.2 Chemical Synthesis

Cetyltrimethylammonium Bromide (CTAB) coated GNRs samples were synthesized by exactly following the steps described in the literature [5]. The UV-visible absorption spectra of the synthesized samples were measured by using a LAMBDA 35 UV/VIS spectrometer (Perkin Elmer Inc.), monitoring over the wavelength range from 400 nm to 1000 nm, in steps of 1 nm.

3. Results & Analysis

3.1 Numerical benchmarking of the Algorithm

Due to the difficulties in obtaining a statistically accurate AR distribution of the GNRs in a sample using transmission electron microscopy (TEM) images, due to smaller numbers of GNRs being available in a single frame of the image, resulting in the inability of distinguish GNRs from substrate effects [3], the developed algorithm was numerically benchmarked. The contribution of ARs of value between 2.5 and 3.5 (in steps of 0.1) were randomly generated using MATLAB and the corresponding generated absorption spectra were input to the algorithms used, to test whether they can correctly retrieve the randomly generated contribution or not. Figure 1(a) enables a cross comparison of the randomly generated contributions, with algorithmically retrieved bounded and unbounded contributions. It can be seen from the figure that these algorithmically retrieved contributions matches well with those that are randomly generated. However, the unbounded case gives negative (i.e. non-physical) contributions for $2 < \text{AR value} < 2.4$, as highlighted in Figure 1(b). This drawback in the unbounded algorithm was overcome by considering the outcome of the bounded algorithm, which predicts the correct contributions throughout its use.

3.2 Determination of AR distribution of chemically synthesized sample

During benchmarking, it was shown that the bounded algorithm predicted the contribution correctly; therefore the same approach was used to obtain the AR contribution in two local, chemically synthesized

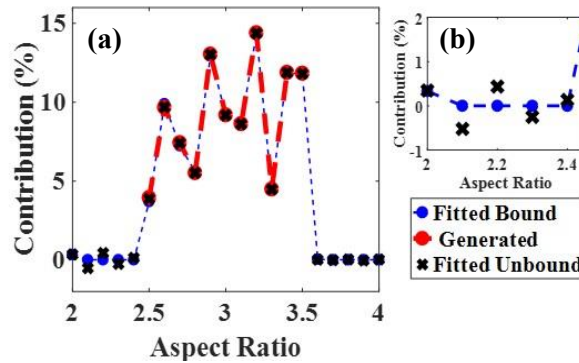


Figure 1: (a) Cross-comparison of the numerically generated contribution with algorithmically-obtained unbounded and bounded contributions. (b) The zoomed portion where least square fitting (unbounded) gives negative (non-physical) values.

samples. Figure 2(a) shows the experimentally obtained and the corresponding fitted spectrum for sample 1. It can be seen that in the LR regime i.e. where the wavelength is ≥ 615 nm, the fitted curve matches closely with the experimentally obtained curve. Since only high AR GNRs ($AR \geq 2$) are used to obtain the fitted curve, the amount of mismatch between the fitted and experimental curves in the TR regime (shown by the dotted box in Figure 2(a)) gives a qualitative understanding of the amount of low AR GNRs ($1 < AR \leq 2$) and nanoparticles ($AR = 1$) present in the sample. The larger the mismatch, the greater the number of low AR GNRs and nanoparticles present in the solution. Figure 2(b) shows the contribution (as a percentage) for GNRs in the range $2 \leq AR \leq 6$, corresponding to the fitting shown in Figure 2(a). The mean (μ) AR value of the solution is 3.4, with a standard deviation (σ) of 0.6.

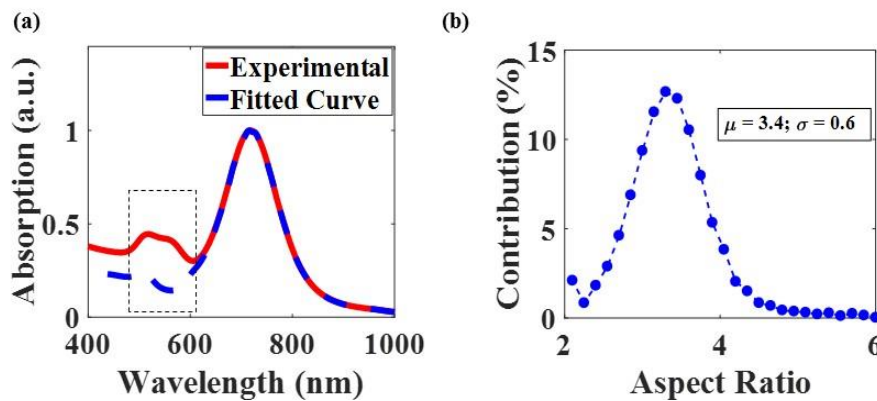


Figure 2: (a) The experimental (solid line) and fitted curve (dotted) obtained in the case of sample 1. The dotted box highlights the transverse plasmon resonance regime. (b) The corresponding aspect ratio distribution obtained after fitting the experimental longitudinal plasmon resonance peak. The legend shows the mean (μ) and the standard deviation (σ) of the obtained aspect ratio.

Figure 3(a) shows the experimentally obtained and corresponding fitted curve for sample 2. In the LR region both are seen to match well. However, the mismatch between the fitted and the experimental spectrum is very large in the TR regime, thus indicating the abundance of low AR GNRs and nanoparticles present in the sample. Figure 3(b) shows the AR distribution corresponding the fitted curve shown in Figure 3(b). From this it can be seen that the mean (μ) the AR of the solution is 3.8, with a standard deviation (σ) of 1.1.

4. Discussion

The algorithm that has been developed in this work, using Bellman Principle of Optimality has, after numerical benchmarking been applied, been used to determine the AR distribution of two locally synthesized samples. The results that have been obtained from the analysis show that the fitted curve closely matches the experimentally obtained spectrum in the LR regime and thus can be used rapidly to determine the AR distribution of GNRs in a chemically synthesized colloidal solution. The mismatch between the fitted and the experimental curves in the TR regime can further be used to allow a qualitative estimate of the low ARs GNRs and gold nanoparticles in the sample.

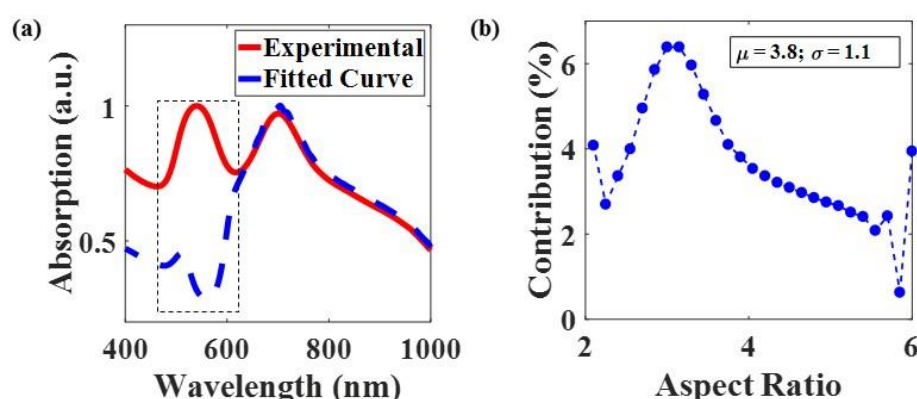


Figure 3: (a) The experimental and fitted curve obtained in case of sample 2. The dotted box highlights the mismatch between them in the transverse plasmon resonance regime. (b) The Aspect ratio distribution obtained corresponding to the fitted curve. Legend shows the mean (μ) and standard deviation (σ) of the distribution.

Acknowledgements

Rahul Kumar is pleased to acknowledge support from the Worshipful Company of Tin Plate Workers *alias* Wire Workers of the City of London by way of a Travelling Fellowship to present this paper. The support of the Royal Academy of Engineering and the George Daniels Educational Trust is also gratefully appreciated.

References

- [1] Hu, M., Chen, J., Li, Z. Y., Au, L., Hartland, G. V., Li, X. & Xia, Y. (2006). Gold nanostructures: engineering their plasmonic properties for biomedical applications. *Chem. Soc. Rev* **35** 1084-1094.
- [2] Burrows, N. D., Lin, W., Hinman, J. G., Dennison, J. M., Vartanian, A. M., Abadeer, N. S., & Murphy, C. J. (2016). Surface chemistry of gold nanorods. *Langmuir* **32** 9905-9921.
- [3] Eustis, S., & El-Sayed, M. A. (2006). Determination of the aspect ratio statistical distribution of gold nanorods in solution from a theoretical fit of the observed inhomogeneously broadened longitudinal plasmon resonance absorption spectrum. *J. Appl. Phys* **100** 044324.
- [4] Das, S. (2011). Binary solutions for overdetermined systems of linear equations. *arXiv preprint arXiv:1101.3056*.
- [5] Jang, B., Park, J.Y., Tung, C.H., Kim, I.H. and Choi, Y., 2011. Gold nanorod– photosensitizer complex for near-infrared fluorescence imaging and photodynamic/photothermal therapy in vivo. *ACS Nano* **5** 1086-1094.